Ignition Dynamics of Fully Reactive Propellant in Stagnation Flow

A. Birk*
Ballistic Research Laboratory, Aberdeen Proving Ground, Maryland

The ignition dynamics of a reactive homogeneous propellant immersed in a hot, reactive, low subsonic flow is solved numerically for the stagnation point. The solution includes the entire ignition process from the onset of the flow to the attainment of steady burning under steady flow. The gas phase equations are of the nonsteady boundary-layer type, including freestream nonsteadiness. The reactive gas phase is coupled to the reactive condensed phase which has reactant depletion and surface regression. Ignition delay times and dynamics are calculated for variations in flow velocity, pressure, temperature, freestream oxidizer content, condensed phase activation energy and heat of reaction, and initial propellant temperature. The transition from one steady burning state to another after a pressure pulse is also investigated. Conditions are identified when dominance shifts from the condensed phase to the gas phase. Excursions of the condensed phase reaction front cause fluctuations of the surface temperature (hence, regression rates) before steady burning. In marginal cases (e.g., low initial propellant temperature), the excursions trigger a low-frequency, ignition-extinction sequence.

Nomenclature

A_p = pre-exponent factor of pyrolysis rate expression, cm/s
A_R = pre-exponent factor of gas phase reaction rate expression, cm^3/g-s
A_S = pre-exponent factor of solid phase reaction rate expression, 1/s
C_P = specific heat capacity, cal/g-K
D_G = gas Damkohler number, defined by Eq. (2a), n-d
E_P = pyrolysis activation energy, cal/mole
E_R = gas phase activation energy, cal/mole
E_S = solid phase activation energy, cal/mole
K = thermal conductivity, cal/cm-s-K
L_V = heat of gasification (endothermic), cal/g
n = stoichiometric ratio
P = pressure, MPa
Q = total heat of combustion of propellant, cal/g
Q_R = gas phase heat of reaction, cal/g
Q_S = solid phase heat of reaction, cal/g
R = radius of curvature of propellant surface, cm
$\mathcal{R}$ = universal gas constant, cal/mole-K
t = time, s
T = temperature, K
T_{ef} = maximum freestream temperature, K
u = velocity component tangential to the surface, m/s
U_E = freestream velocity, m/s
V_{REG} = regression velocity of the propellant surface, cm/s
$\dot{W}$ = volumetric rate of production of a species, g/cm^3-s
$\dot{W}_S$ = rate of solid molecules decomposition, 1/s
x = coordinate tangential to the wall, cm
y = coordinate normal to the wall, cm
Y = mass fraction of a species
α = fractional mass of fuel constituent of propellant
μ = viscosity, g/cm-s
ρ = density, g/cm^3

Subscripts

e = at the boundary-layer edge
E = at the stagnation point freestream
F = fuel
I = interior of propellant
OX = oxidizer
P = products
S = solid phase
W = wall (surface)
∞ = at infinity

Received Dec. 16, 1981; revision received April 30, 1982. Copyright © American Institute of Aeronautics and Astronautics, Inc., 1982. All rights reserved.

*NRC Research Associate, ARRADCOM. Member AIAA.

Introduction

COMBUSTION anomalies in guns have been traced to ignition problems.[1] One possible mechanism for combustion difficulties is a sudden gas phase ignition if the propellant "fizzes" without burning and the partially decomposed products fill the chamber. Another possibility is that the transition from ignition to burning is unstable or oscillatory. This work investigates the dynamics of gun-like, ignition-combustion transition where ignition is convective and the propellants are nitrocellulose based. Such propellants are known to be reactive in their condensed phase.[2,3] This study treats stagnation flow ignition because the stagnation region is a favorable site for ignition.[4]

The ignition terminology distinguishes between solid phase ignition and gas phase ignition. In the latter case, the condensed phase need not be reactive and ignition foretells the appearance of flame. In the former case (thermal ignition theories), nothing is said about flame development, although most of the propellant energy is released in the flame. In the combustion literature no attention has been given to the links between solid-gas phase ignition in relation to flame development and transition to burning. Theoretical treatment of the solid phase ignition of propellant in stagnation flow is given by Niioka and Williams[5] and it is corroborated by the experiments of Niioka et al.[6] However, these studies do not treat the transition to burning and are limited to situations when condensed phase ignition is predominant. Numerical analysis of gas phase ignition of propellants in stagnation flow is given by Birk and Caveny.[4] The present study extends the analysis to situations when there is no clear distinction between gas and solid phase ignition. The numerical solution follows the ignition transition well into the period of propellant burning. In particular, a subsurface exothermic reaction depletion is treated.

The structure and propagation of a reactive front in gasless systems have been studied extensively.[7,8] An important finding is that for some thermochemical values the front structure and propagation speed oscillate. Such oscillation may be important when coupled to the regressing propellant surface and the gas phase. For burning propellants, the reaction front is attached to the regressing surface.

The subsurface reaction of burning solid propellants is often treated as collapsed at the surface.[9,10] The exothermicity of this reaction is responsible for unstable burning under steep pressure variation. In the ignition situation, the overall gasification of the propellant (including its subsurface reaction) may start endothermic and become exothermic as the surface temperature rises. The variation of the overall energy balance of the gasification (with the surface temperature and the subsurface reaction completeness) may be a cause for unstable transition to burning even under constant pressure. This study addresses such a possibility.

Analysis

The formulation is given for the general case of time variant stagnation flow over an axisymmetric body composed of a homogeneous solid propellant. The flow is low subsonic and has imposed variations of acceleration, pressure, and temperature. The propellant decomposes into fuel and oxidizer species when heated. Chemical reactions occur both in the condensed phase and in the gas phase leading eventually to ignition and combustion. It is a boundary-layer flow analysis.

Gas Phase Equations

Considering the lack of knowledge of the exact chemical kinetics, and in order to simplify the equations yet retain their main features, the following assumptions are made.

1) The specific heat is the same for all gaseous species and is constant.

2) The molecular weights and diffusion coefficients are the same for all species.

3) The Prandtl, Schmidt, and Lewis numbers are unity.

4) $\rho\cdot\mu/\rho_e\cdot\mu_e=1$ everywhere in the flowfield.

5) One step global chemical reaction which follows second-order Arrhenius kinetics, of the form:

$$[\text{fuel}]+n\cdot[\text{oxidizer}]=(n+1)\cdot[\text{products}]$$

$$\dot{W}_F=-\rho^2 A_R\cdot Y_F\cdot Y_{OX}\cdot\exp(-E_R/\Re T)$$

A single reaction can be rationalized by considering the *hot thin* boundary-layer flow. The typical three reaction zones (fizz, dark, and luminous flame) observed in *strand burners*[3] are now merged. The boundary layer is much thinner than the dark zone and the temperature at its edge is higher.

6) The freestream velocity is $u_e=a\cdot U_E(t)\cdot x$ where a is some constant.

The residence time of the flow is

$$t_f=[(1+j)\cdot a\cdot U_E]^{-1} \tag{1}$$

where $j=0$ for two dimensions, $j=1$ for three dimensions, and it is incorporated in the following Damkohler number.

$$D_G=t_f\cdot\rho_e\cdot(T_E/T_{ef})\cdot A_R \tag{2a}$$

The following parameters are defined.

$$h=Q_R/C_P T_{ef} \qquad \Theta_R=E_R/\Re T_{ef} \tag{2b}$$

The independent variables are transformed as follows.

$$\eta=\frac{1}{(t_f\cdot\rho_e\mu_e)^{1/2}}\cdot\int_0^y\rho\,dy \qquad \tau=\int_0^t t_f^{-1}dt \tag{3}$$

and new dependent variables are defined

$$F=-\left(\frac{t_f}{\rho_e\mu_e}\right)^{1/2}\cdot\rho_S\cdot V_{REG}+\int_0^\eta\frac{u}{u_e}d\eta$$

$$H=\theta+(h/n)\,Y_{OX} \qquad \text{where} \qquad \theta=T/T_{ef}$$

$$Z=Y_{OX}-nY_F \tag{4}$$

The two last definitions convert the boundary-layer equations into a Schvab-Zeldovich form.

$$G=\frac{\partial F}{\partial\eta}$$

$$-\frac{\partial G}{\partial\tau}+\frac{\partial^2 G}{\partial\eta^2}+F\frac{\partial G}{\partial\eta}=(1+j)^{-1}\cdot\left(G^2-\theta\frac{T_{ef}}{T_E}\right)$$

$$+t_f\frac{d\ell n U_E}{dt}\cdot\left(G-\theta\frac{T_{ef}}{T_E}\right)+\frac{t_f}{2}\cdot\frac{d\ell n(U_E/P_E)}{dt}\cdot\eta\cdot\frac{\partial G}{\partial\eta} \tag{5}$$

$$-\frac{\partial Z}{\partial\tau}+\frac{\partial^2 Z}{\partial\eta^2}+F\cdot\frac{\partial Z}{\partial\eta}=\frac{t_f}{2}\cdot\frac{d\ell n(U_E/P_E)}{dt}\cdot\eta\cdot\frac{\partial Z}{\partial\eta} \tag{6}$$

$$-\frac{\partial H}{\partial\tau}+\frac{\partial^2 H}{\partial\eta^2}+F\cdot\frac{\partial H}{\partial\eta}=\frac{t_f}{2}\cdot\frac{d\ell n(U_E/P_E)}{dt}\cdot\eta\cdot\frac{\partial H}{\partial\eta}$$

$$-\frac{t_f}{C_P\rho_e T_E}\cdot\frac{dP_E}{dt}\cdot\theta-(H-\theta)\cdot\frac{\partial\ell n h}{\partial\tau} \tag{7}$$

$$-\frac{\partial\theta}{\partial\tau}+\frac{\partial^2\theta}{\partial\eta^2}+F\cdot\frac{\partial\theta}{\partial\eta}$$

$$=-\left[(H-\theta)\frac{n}{h}-Z\right]\cdot\frac{H-\theta}{\theta}\cdot D_G\exp\left(-\frac{\Theta_R}{\theta}\right)$$

$$+\frac{t_f}{2}\cdot\frac{d\ell n(U_E/P_E)}{dt}\cdot\eta\cdot\frac{\partial\theta}{\partial\eta}-\frac{t_f}{C_P\rho_e T_E}\cdot\frac{dP_E}{dt}\cdot\theta \tag{8}$$

Solid Phase Equations

The following are assumed: 1) the heat transfer is one dimensional; 2) a subsurface chemical reaction of first order $\dot{W}_S=-A_S\cdot Y_S\cdot\exp(-E_S/\Re T_S)$; 3) species diffusion is neglected.

The following parameters are defined.

$$D_W=t_f\cdot\frac{\rho_S^2}{\rho_e u_e}\cdot A_P^2 \qquad D_S=t_f\cdot A_S$$

$$\gamma=\frac{C_{PS}}{C_P} \qquad \epsilon=\frac{\rho_S K_S C_S}{\rho_e K_e C_P} \qquad h_S=\frac{Q_S}{C_{PS}T_{ef}}$$

$$\Theta_S=\frac{E_S}{\Re T_{ef}} \qquad \Theta_P=\frac{E_P}{\Re T_{ef}} \tag{9}$$

The independent variables are transformed as follows.

$$\eta_S=\left(\frac{\rho_S C_{PS}}{K_S t_f}\right)^{1/2}\cdot y_S \qquad \tau=\int_0^t t_f^{-1}dt \tag{10}$$

The dependent variables are Y_S and

$$\theta_S=T_S/T_{ef} \tag{11}$$

The following solid phase equations are obtained.

$$-\frac{\partial\theta_S}{\partial\tau}+\frac{\partial^2\theta_S}{\partial\eta_S^2}+\left[\left(\frac{D_W}{\epsilon}\right)^{1/2}\cdot\gamma\cdot\exp\left(-\frac{\Theta_P}{\theta_W}\right)\right.$$

$$\left.-\frac{t_f}{2}\cdot\frac{d\ell n U_E}{dt}\cdot\eta_S\right]\frac{\partial\theta_S}{\partial\eta_S}=-h_S\cdot D_S\cdot Y_S\cdot\exp\left(\frac{\Theta_S}{\theta_S}\right) \tag{12}$$

$$-\frac{\partial Y_S}{\partial\tau}+\left[\left(\frac{D_W}{\epsilon}\right)^{1/2}\cdot\gamma\cdot\exp\left(-\frac{\Theta_P}{\theta_W}\right)\right.$$

$$\left.-\frac{t_f}{2}\cdot\frac{d\ell n U_E}{dt}\cdot\eta_S\right]\cdot\frac{\partial Y_S}{\partial\eta_S}=D_S\cdot Y_S\cdot\exp\left(-\frac{\Theta_S}{\theta_S}\right) \tag{13}$$

Boundary Conditions

The boundary conditions reflect the nonslip condition, the blowing at the surface, the conservation of heat and mass at the surface, and conditions at the gas phase boundary-layer edge and solid phase interior. In particular, the following is assumed.

1) The regression rate is expressed by an Arrhenius pyrolysis law and it depends only on the surface temperature.

$$V_{\mathrm{REG}} = A_P \cdot \exp(-E_P/\Re T_W)$$

2) The solid phase pyrolyzes at the surface to fuel and oxidizer with fractional mass ratios of α and $1-\alpha$.

3) The gasification at the surface of the unreacted portion of the solid is endothermic. The transition to the gas phase of the reacted portion of the solid phase is thermoneutral.

4) The overall energy of the propellant is fixed; therefore, as more energy is released in the solid phase, less of it is available in the gas phase.

Assumptions 1-3 comprise a new treatment of the regression chemistry. It is often hypothyzed that the initial stage of nitrocellulose propellant decomposition is

$$R-\mathrm{ONO_2} \rightarrow \mathrm{NO_2} + \mathrm{R'-CHO\ species}$$

which is endothermic ($\sim$35 kcal/mole). $R-\mathrm{ONO_2}$ represents the unreacted portion of the solid. Being a large molecule $R-\mathrm{ONO_2}$ is pyrolyzed at the surface, with inital stage as shown earlier, to various gaseous species. If the subsurface temperature is high enough, some decomposition takes place in the solid and $\mathrm{NO_2}$ reacts exothermically

$$\mathrm{NO_2} + \mathrm{R'-CHO} \rightarrow \mathrm{products}$$

The products are the reacted portion of the solid. Since less than 10% of the propellant total energy is released in the preceding reaction, most of the products are probably large solid molecules resembling the unreacted ones. If so, the fuel-oxidizer ratio α is essentially unchanged and the same regression law always applies. The products pyrolysis at the surface is assumed thermoneutral since the $\mathrm{NO_2}$ bond is already broken.

There is no direct evidence for the mechanism described; however, there is experimental evidence that the solid-gas transition in nitrocellulose based propellants is overall exothermic when the surface temperature is high.[3] If the surface gasification is assumed to be exothermic, unrealistic short ignition delay times are obtained. If it is assumed to be endothermic, unrealistic surface temperatures during ignition are obtained (when adhering to an overall exothermic transition).

The initial conditions are quiescence at time $t=0$ and some given step function of freestream conditions at time $t=0^+$. Thereafter, the freestream conditions vary with time in a given manner.

The boundary conditions are as follows.

$\tau=0$	$G=1$	$\tau=0^+$	$G=1$
$\eta\geq 0$	$\theta=T_{EI}/T_{ef}$	$\eta\geq 0$	$\theta=T_E/T_{ef}$
$(\eta_S\geq 0)$		$(\eta_S\geq 0)$	
	$Z=Y_{\mathrm{OX}E}$		$Z=Y_{\mathrm{OX}E}$
	$H=\dfrac{T_{EI}}{T_{ef}}+\dfrac{h}{n}Y_{\mathrm{OX}E}$		$H=\dfrac{T_E}{T_{ef}}+\dfrac{h}{n}Y_{\mathrm{OX}E}$
	$\theta_S=\dfrac{T_{SI}}{T_{ef}}$		$\theta_W=\dfrac{1+\theta_{SI}\cdot\epsilon^{1/2}}{1+\epsilon^{1/2}}$
	$Y_S=1$		(14a)

$\tau\geq 0^+$ $\quad G_W=0$

$\eta=0$ $\quad F_W=-(D_W)^{1/2}\cdot\exp\left(-\dfrac{\Theta_P}{\theta_W}\right)$

$(\eta_S=0)$ $\quad \left(\dfrac{\partial Z}{\partial\eta}\right)_W+F_WZ_W=\left[1-\alpha(1+n)\cdot\dfrac{h}{n}\right]\cdot F_W$ (14b)

$$\left(\frac{\partial H}{\partial\eta}\right)_W+F_WH_W=\left(\frac{\partial\theta}{\partial\eta}\right)_W+\left[\theta_W+(1-\alpha)\cdot\frac{h}{n}\right]\cdot F_W-\left(\frac{\partial\theta}{\partial\eta}\right)_W-\epsilon^{1/2}\cdot\left(\frac{\partial\theta_S}{\partial\eta_S}\right)_W=g\cdot F_W\cdot Y_{SW} \quad (14b')$$

where

$$g=L_V/C_PT_{ef}$$

$\tau\leq 0^+$ $\quad G_\infty=1$

$\eta=\infty$ $\quad \theta_\infty=T_E/T_{ef}$

$(\eta_S=\infty)$ $\quad Z=Y_{\mathrm{OX}E}$

$$H=\frac{T_E}{T_{ef}}+\frac{h}{n}Y_{\mathrm{OX}E}$$

$$\theta_S=T_{SI}/T_{ef}$$

$$Y_S=1 \qquad (14c)$$

In addition [for Eq. (2b)],

$$Q_R=(Q+L_V)\left[1-\frac{Q_S+L_V}{Q+L_V}(1-Y_{SW})\right] \qquad (14d)$$

Solution

The equations were solved numerically using a generalized implicit scheme. The finite difference elements form block tridiagonal matrices for Eqs. (5-8) and Eqs. (12) and (13). A variable time step accommodated the various time scales of the problem. The nonlinear terms were linearized around predicted values and the solution was iterated until convergence. To render Eq. (14b) linear, an estimated θ_W was used in all the equations and Eq. (14b') dropped. The equations were then solved iteratively until Eq. (14b') was satisfied.

The solution includes the boundary-layer development and the transition from ignition to steady-state burning. The initial profiles were derived as by Strahle.[11] To accommodate the variation in the boundary-layer thickness, and yet keep fine resolution of the gas phase difference grid, the size and number of the mesh cells were varied during the solution execution. To get good accuracy for the heat transfer and subsurface reaction, a fine grid has to be used near the wall; yet the same grid has to cover the entire depth of the thermal wave. Therefore, the coordinate η_S was transformed logarithmically to a new coordinate in Eqs. (12) and (13).

The boundary condition for Y_{SW} was given on a characteristic line; thus, the time step was bounded by the Courant condition. The relative orders of magnitude of the left-hand side terms in Eq. (13) were checked constantly. By neglecting either of them, the Courant time step requirement was relaxed at the beginning and end of the ignition solution.

The solution accuracy was checked by varying the size of the time steps, mesh size, and the value of the implicit split

parameter ($\hat{\theta}$). The solution was found to be stable for $\hat{\theta} = 0.7$-1 (0, full explicit; 1, full implicit).

Results

The solution is for the stagnation flow over a cylinder (two-dimensional flow) because the cylinder is the common practical configuration. The solution for three-dimensional flow does not differ much from that for two dimensional. The physochemical values and the nominal flow conditions assumed are specified in Table 1. The values fall within the range of the experimental data for nitrocellulose based propellants. Since about half the weight of a typical propellant is oxygen, α is chosen to be 0.5. Since half oxygen is still fuel rich (about -35% oxygen balance), n is chosen to be 2 and fuel is available to react with freestream oxidizer. Indeed, the solution yields ignition delay times, surface burning temperatures, and regression rates which agree with the experimental data of Refs. 3, 4, and 12. In particular, the kinetics and exothermicity of the condensed phase were chosen to: 1) predispose neither solid nor gas phase ignition for the nominal flow conditions, and 2) result in a reaction zone attached to the regressing surface.

Table 1 Values of physical properties used in calculations

K_e, cal/cm-s-K	0.000247
ρ_e, g/cm^3	0.00314
C_{P_e}, cal/g-k	0.285
μ_e, g/cm-s	0.000901
K_S, cal/cm-s-K	0.00015
ρ_S, g/cm^3	1.54
C_{P_S}, cal/g-K	0.35
α	0.5
n	2
A_R, cm^3/g-s	10^{10}
A_S, 1/s	10^{14}
A_P, cm/g	10^5
E_R, kcal/mole	14
E_S, kcal/mole	30
E_P, kcal/mole	16
Q, cal/g	1380
Q_S, cal/g	80
L_V, cal/g	120
U_E, m/s	10
T_E, K	1500
P_E, MPa	1.72
T_{SI}, K	300
R, cm	0.35

Ignition Paths

The main mechanisms for convective ignition are depicted in Fig. 1. Time is from the onset of flow and heat flux is at the surface on the gas side. Ignition is not easily distinct on either curve 1 or 3 but is pronounced on curve 4; thus, there is no clear distinction here between solid or gas phase ignition. The following describes the events on curve 4.

When the propellant is immersed suddenly in the hot gas, the heat flux is initially infinite; thus, the surface temperature jumps to some higher value [Eq. (14a)]. During the boundary-layer development ($\sim t_f$), the heat flux becomes finite. The stage of inert heating (including endothermic gasification) lasts until time A (Fig. 1). Then, the heat feedback from the exothermic gas reaction becomes significant. At time B, the heat flux starts to rise despite the rise in surface temperature and blowing of gas from the surface. This is the first sign of gas phase ignition. At time C, the solid phase reaction becomes significant. At this stage the heat production in the solid exceeds the heat losses to the solid interior; the surface temperature rises rapidly as does the concentration of the decomposition products in the gas phase. The heat feedback from the gas phase increases and drives the surface temperature higher. At time D, the blowing effect starts to decrease the heat feedback. At time E, the reactive species in the solid phase is fully consumed and the surface temperature overshoots. The surface temperature then subsides due to heat dissipation into the solid. Excursions of the subsurface reaction front during the transition to steady state (E-F) are responsible for the fluctuations in the surface temperature (and, thus, in the burning rate). The ignition is considered to be less stable if these fluctuations are slow decaying and have large amplitudes. At the extreme, a situation of an ignition-extinction cycle may occur. The subsurface structures at times E and F are shown in Fig. 2. A solution which considered the solid reaction to be collapsed at the surface yielded no surface temperature fluctuations after time E.

In Fig. 1, the point B coincides with the minimum heat flux point (B′) on curve 1. If B′ occurs more than a C-D time interval *before* C, the ignition is considered gas phase. If B′ is more than C-D *after* C, the ignition is solid phase. The time B′ depends on the Damkohler number D_G; B′ occurs sooner to C for a larger D_G. If D_G is small enough B′ may never occur[4] and the surface temperature curve would resemble curve 3 (no flame).

Effects of Freestream Conditions

The variations of the ignition delay and surface temperature with velocity for inert and for oxidizer flow are shown in Fig. 3 (ignition delay is defined as the time to reach the first overshoot of the surface temperature, i.e., point E in Fig. 1). The shorter ignition delay for higher velocity is due to higher heat transfer to the surface in the inert stage of ignition. Ignition delay, however, has a minimum since when the velocity is high enough (i.e., small D_G), ignition does not occur.[4] Figure 4 indicates that when ignition delay is longer, the surface temperature further overshoots its steady-state value. This trend is explained as follows. When ignition delay is longer, the thermal wave in the solid is thicker and so is the subsurface reaction zone; therefore, when the solid reaction peaks, heat production exceeds conduction. This trend is also apparent in Figs. 4 and 5. Figure 4 depicts the effects of freestream temperature. As expected, the ignition delay decreases for higher freestream temperature. As the temperature increases both heat transfer and reaction rate increase and there is no minimum ignition delay. Ignition delay also decreases for higher pressure which is also an experimental finding.[4]

The steady-state surface temperature does not vary with velocity, freestream oxidizer (Fig. 3), or temperature (Fig. 4). The key is the steady-state boundary-layer structure (Fig. 6). It is the primary reaction zone (RR) near the surface that provides the heat feedback for sustained burning. When freestream temperature increases or velocity decreases, the boundary layer thickens; but in both cases the reaction rate increases to keep heat transfer to the surface (and, thus, the surface temperature) almost unchanged. In contrast, when the boundary layer thickens at a lower pressure, the reaction rate decreases and the heat transfer to the surface (and, thus, the surface temperature) decreases significantly (Fig. 5). The freestream oxidizer participates in the reaction near the surface only during the early stage of ignition and, thus, shortens its delay (Fig. 3). However, when steady state approaches, a secondary reaction zone (for a fuel rich propellant) is formed far from the surface and contributes only little heat feedback (see Refs. 4 and 13).

Ignition Stability

The oscillatory decay of the surface temperature overshoot to steady state does not depend on the ignition delay. For higher velocities the ignition is less stable; the surface temperature fluctuations decay slower. Also, the oscillation frequency becomes lower. Higher freestream temperature has little effect on the decay time and frequency. However, the decay is faster and its frequency higher when ignition is under higher pressures. Noteworthy is that a pure gas phase solution may yield surface temperature overshoot but the decay to

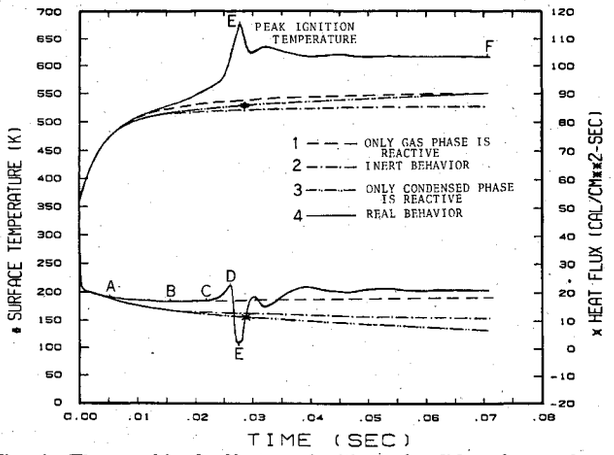

Fig. 1 The combined effect on ignition of solid and gas phase reactivities.

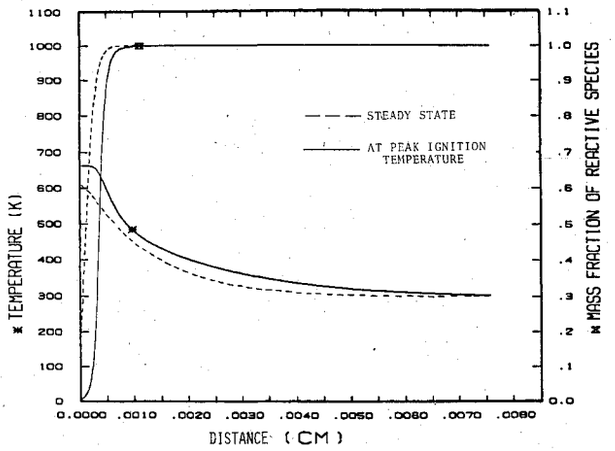

Fig. 2 Subsurface structure: the excursion of the subsurface reaction front.

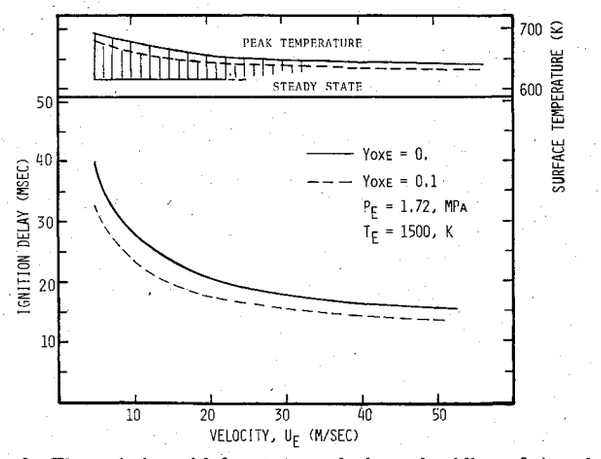

Fig. 3 The variation with freestream velocity and oxidizer of a) peak surface temperature at ignition and its delay and b) steady-state burning surface temperature.

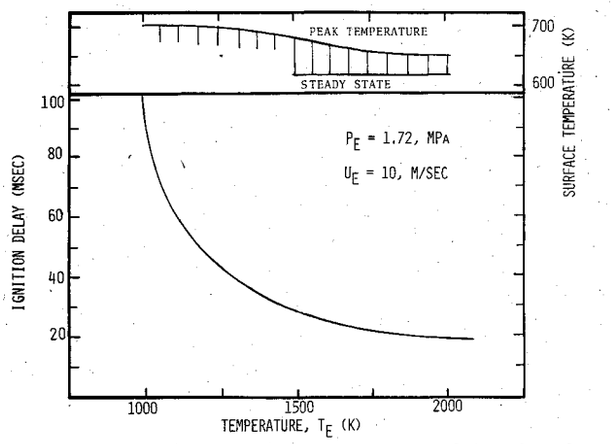

Fig. 4 The variation with freestream temperature of a) peak surface temperature and its delay and b) steady-state burning surface temperature.

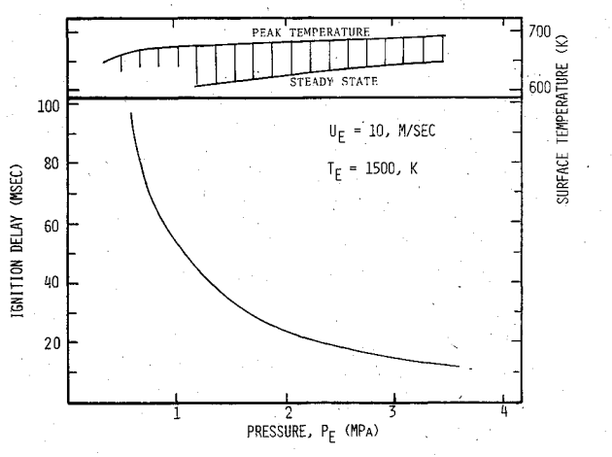

Fig. 5 The variation with pressure of a) peak surface temperature and its delay and b) steady-state burning surface temperature.

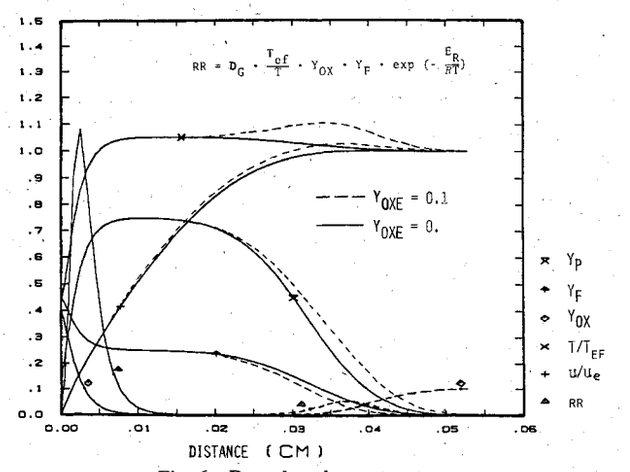

Fig. 6 Boundary-layer structure.

steady state is fast and monotonic. Therefore, lower stability implies the inability of the gas phase alone to sustain burning. For higher velocities the flame is less stable and will tend to blow off (low D_G) when disturbed by excursions in the solid phase reaction. When the ignition curves in Fig. 7 are extrapolated to higher velocities, the surface temperature peaks below the steady state and extinction occurs. Another finding is that for steady-state burning at higher pressure, the overall solid phase exothermicity drops (and heat feedback from the gas rises). Thus, at higher pressure, dominance is shifted to the gas phase and stability is increased.

Pressure Unsteadiness

The effects of steep pressure gradients on steady-state burning are investigated for two cases: pressurization (Fig. 8) and depressurization (Fig. 9). The pressure gradient is in the form $\Delta P = \Delta P_{\max} \cdot [1-(\beta \cdot t+1)\cdot \exp(-\beta \cdot t)]$. A value of $\beta = 50/t_f$ was used; thus, the pressure variation distorts momentarily the boundary-layer structure which results in

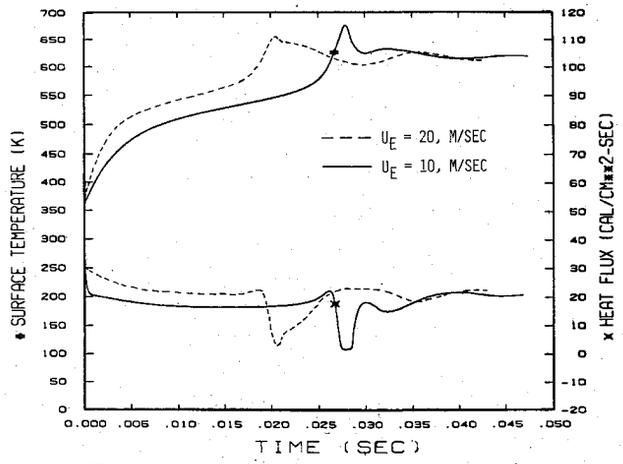

Fig. 7 Effects of freestream velocity on ignition.

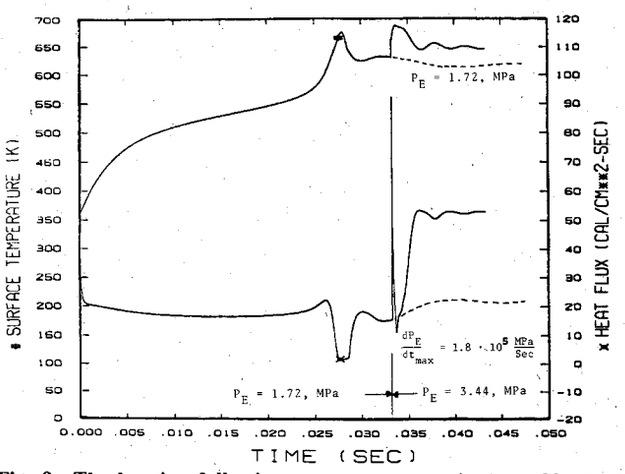

Fig. 8 The burning following a steep pressure rise resembles that which follows the ignition at the higher pressure.

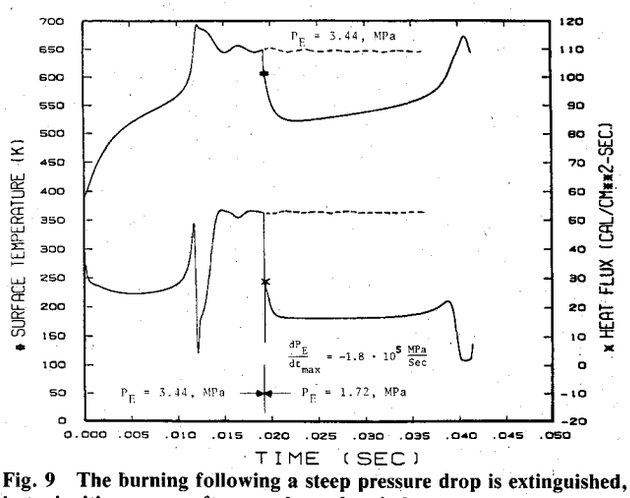

Fig. 9 The burning following a steep pressure drop is extinguished, but reignition occurs after a prolonged period.

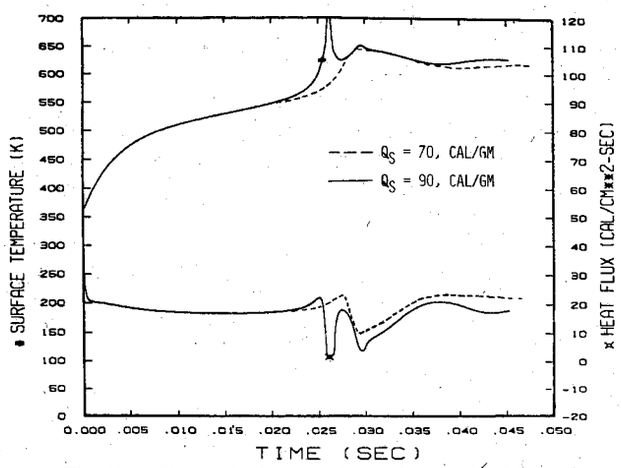

Fig. 10 Effects of subsurface heat release on ignition.

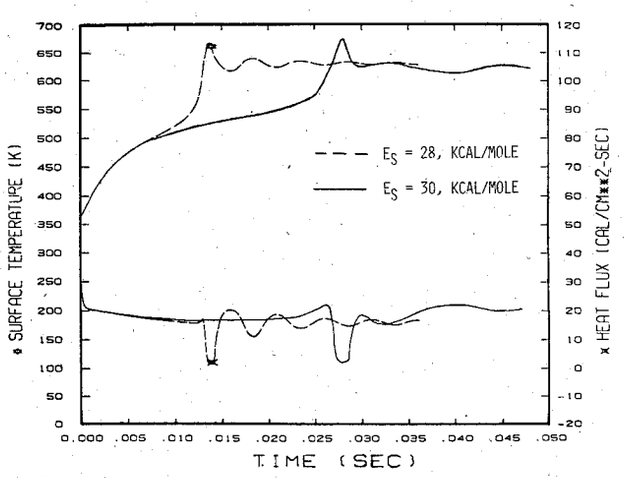

Fig. 11 Effects of solid phase activation energy on ignition.

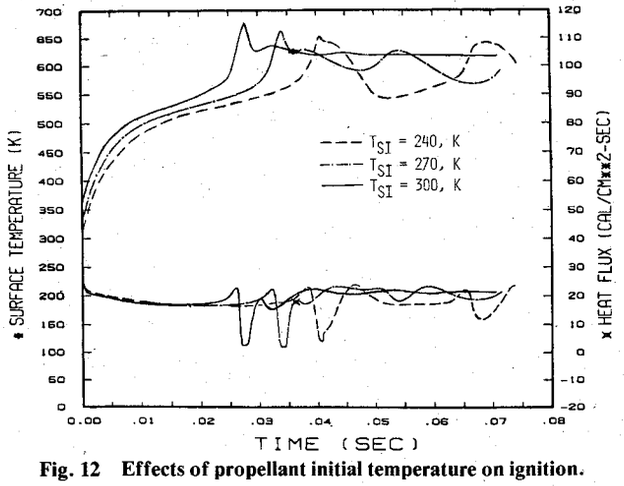

Fig. 12 Effects of propellant initial temperature on ignition.

heat transfer overshoot (pressurization) and undershoot (depressurization). The burning following the pressurization (Fig. 8) resembles that which follows the ignition at the higher pressure (Fig. 9). The depressurization results in instant extinction and then reignition after a prolonged period. The reignition curve resembles the ignition curve at the lower pressure (Fig. 8). Thus, the conclusion is that pressure unsteadiness does not introduce new burning instabilities that do not exist in the ignition processes under steady pressures.

Velocity unsteadiness, on the other hand, has little effect on steady-state burning. This is not surprising since the burning surface temperature (and, hence, the thermal wave thickness) is unchanged over the range of velocities considered.

Effects of Solid Phase Parameters

The effects of thermal and chemical parameters of the gas phase are described by Ref. 4. Solid phase parameters which influence the results are subsurface activation energy, heat of reaction, and initial temperature. Higher heat of reaction markedly increases peak surface temperature (Fig. 10). It also

increases the frequencies of surface temperature excursions. This frequency also increases when the activation energy is lower (Fig. 11). The fraction of unreacted solid at the surface (Y_{SW}) fluctuates during the subsurface reaction front excursions (Fig. 2). The endothermic gasification of this unreacted solid [Eq. (14b′)] absorbs heat from the solid and, therefore, lowers the excursion frequency. At lower activation energy (28 kcal/mole) Y_{SW} is zero during the excursions; thus, their frequency is higher. When the initial temperature (T_{SI}) is low enough (240 K) Y_{SW} reaches high values during the excursions which results in a low-frequency, extinction-ignition cycle (Fig. 12). A solution, assuming thermoneutral gasification [i.e., $g=0$ in Eq. (14b′)], yields smooth ignition and burning even for lower T_{SI}. The thermoneutral gasification assumption has no effect on the solution for the lower activation energy since there $Y_{SW}=0$.

Conclusions

For stagnation flow ignition and combustion the following are the conclusions of this study.

1) The transition from ignition to steady-state burning is smoother when the gas phase dominates ignition (e.g., high pressures, low velocities).

2) Excursions of the solid reaction front cause unstable ignition.

3) When neither gas phase nor solid phase dominates ignition, the surface temperature during ignition overshoots its steady-state value when ignition delay is longer or subsurface heat of reaction is higher.

4) Ignition is less stable when the initial propellant temperature is lower.

5) Burning instability due to steep pressurization resembles that of ignition at the higher pressure. Depressurization may result in extinction and long delayed reignition.

6) The computed excursions of the surface regression are high enough to be detected. An experimental test of their actuality is needed.

References

[1] May, I.W., White, K.J., Nelson, C.W., and Rocchio, J.J., "The Role of Ignition in Artillery Propulsion," *Proceedings of the Third International Symposium on Ballistics,* Paper A3, March 1977.

[2] Zenin, A.A., "Structure of Temperature Distribution in Steady-State Burning of a Ballistic Powder," *Fizika Goreniya i Vzryva,* Vol. 2, No. 3, 1966, pp. 67-76.

[3] Kubota, N., "Determination of Plateau Burning Effect of Catalyzed Double-Base Propellant," *17th International Symposium on Combustion,* The Combustion Institute, 1978, pp. 1435-1442.

[4] Birk, A. and Caveny, L.H., "Convective Ignition of Propellant Cylinders in a Developing Cross-Flow Field," MAE Rept. 1486, Princeton University, Sept. 1980.

[5] Niioka, T. and Williams, F.A., "Ignition of a Reactive Solid in a Hot Stagnation-Point Flow," *Combustion and Flame,* Vol. 29, No. 1, 1977, pp. 43-54.

[6] Niioka, T., Takahashi, M., and Izumikawa, W., "Ignition of Double Base Propellant in Hot Stagnation Point Flow," *Combustion and Flame,* Vol. 35, No. 1, 1979, pp. 81-97.

[7] Shkadinskii, K.G., Khaikin, B.I., and Merzhanov, A.G., "Propagation of a Pulsating Exothermic Reaction Front in the Condensed Phase," *Fizika Goreniya i Vzryva,* Vol. 7, No. 1, 1971, pp. 19-28.

[8] Matkowsky, B.J. and Sivashinsky, G.I., "Propagation of a Pulsating Reaction Front in Solid Fuel Combustion," *SIAM Journal of Applied Mathematics,* Vol. 35, No. 3, 1978, pp. 465-478.

[9] Krier, H., Tien, J.S., Sirignano, W.A., and Summerfield, M., "Nonsteady Burning Phenomena of Solid Propellants: Theory and Experiments," *AIAA Journal,* Vol. 6, No. 2, 1968, pp. 278-285.

[10] Kooker, D.E. and Nelson, C.W., "Numerical Solution of Solid Propellant Transient Combustion," *Journal of Heat Transfer, Transactions of ASME,* Vol. 101, No. 2, 1979, pp. 359-364.

[11] Strahle, W.C., "A Transient Problem on the Evaporation of a Reactive Fuel," *Combustion Science and Technology,* Vol. 1, No. 1, 1969, pp. 25-33.

[12] Lengelle, G. Duterque, J., Verdier, C., Bizot, A., and Truber, J., "Combustion Mechanisms of Double Base Solid Propellants," *17th International Symposium on Combustion,* The Combustion Institute, 1978, pp. 1443-1451.

[13] Hermance, C.E. and Kumar, R.K., "Gas Phase Ignition Theory for Homogeneous Propellants Under Shock Tube Conditions," *AIAA Journal,* Vol. 8, Sept. 1970, pp. 1551-1558.